International Journal of Biological Macromolecules 111 (2018) 1245–1254

Contents lists available at ScienceDirect

International Journal of Biological Macromolecules

journal homepage: http://www.elsevier.com/locate/ijbiomac

# Hyaluronic acid in Pluronic F-127/F-108 hydrogels for postoperative pain in arthroplasties: Influence on physico-chemical properties and structural requirements for sustained drug-release

M.H.M. Nascimento [a], M.K.K.D. Franco [b], F. Yokaichyia [c], E. de Paula [d], C.B. Lombello [e], D.R. de Araujo [a,*]

[a] Human and Natural Sciences Center, ABC Federal University, Santo André, SP, Brazil
[b] Nuclear and Energy Research Institute, São Paulo, SP, Brazil
[c] Department Quantum Phenomena in Novel Materials, Helmholtz-Zentrum Berlin für Materialien und Energie GmbH, Berlin, Germany
[d] Department of Biochemistry and Tissue Biology, Institute of Biology, State University of Campinas, Campinas, SP, Brazil
[e] Engineering, Modelling and Applied Social Sciences Center, ABC Federal University, Santo André, São Paulo, Brazil

ARTICLE INFO

*Article history:*
Received 16 August 2017
Received in revised form 27 November 2017
Accepted 10 January 2018
Available online 12 January 2018

*Keywords:*
Hyaluronic acid
Pluronics
Hydrogel
Lidocaine
Supramolecular structure

ABSTRACT

In this study, we reported the hyaluronic acid (HA) on supramolecular structure of Pluronic F-127 (PLF-127) and/or Pluronic F-108 (PLF-127) hydrogels, as well as their effects on release mechanisms, looking forward their application as lidocaine (LDC) drug-delivery systems in arthroplastic surgeries. We have studied the HA-micelle interaction using Dynamic Light Scattering (DLS), the micellization and sol-gel transition processes by Differential Scanning Calorimetry (DSC) and Rheology., of PL-based hydrogels and. The presence of HA provided the formation of larger micellar dimensions from ~26.0 to 42.4 nm. The incorporation of HA did not change the micellization temperatures and stabilized hydrogels rheological properties ($G' > G''$), showing no interference on PL-thermoreversible properties. Small-Angle-X-ray Scattering (SAXS) patterns revealed that HA incorporation effects were pronounced for PLF-127 and PLF-108 systems, showing transitions from lamellar to hexagonal phase organization (HA-PLF-127) and structural changes from cubic to gyroid and/or cubic to lamellar. The HA insertion effects were also observed on drug release profiles, since lower LDC release constants ($K_{rel}$ = 0.24–0.41 $mM \cdot h^{-1}$) were observed for HA-PLF-127, that presented a hexagonal phase organization. Furthermore, the HA-PL systems presented reduced *in vitro* cytotoxic effects, pointed out their tendency to self-assembly and possible application as drug delivery systems.



## 1. Introduction

Arthroplasty is a surgical procedure to relieve pain and restore range of motion by realigning or reconstructing a join. Arthroplasties cause severe tissue trauma, leading to intense postoperative pain, making analgesia one of the main procedures to promote patient stability during the post-surgical period. Patients are usually elderly with comorbid diseases and it is important to choose the anesthetic/analgesic regimen that will minimize side effects as well as providing suitable pain relief. Analgesia is typically achieved through bolus doses of short-acting local anesthetics (LAs) and/or with oral analgesics, such as opiates, which are associated with systemic side effects. In this sense, LAs have also been used for regional blocks, inducing operative and/or post-operative analgesia, for the treatment of acute and chronic pain [1].

Lidocaine (LDC) (Fig. 1A) is one of the most widely used LA and considered prototype of amino-amide derivatives. It is a weak base (pKa 7.9) with low water solubility [2] (~0.12 mg/mL) that promotes postoperative pain relief, decreased consumption of anesthetics inhalation and opioids, rapid return of intestinal transit and decreased production of interleukins. The analgesic effect of lidocaine on surgical trauma is due to the neuronal blockade, attenuating the neurogenic response [3,4]. However, the short duration of sensory blockade and its reduced analgesia intensity are still challenges for achieving long-duration pain relief. For this reason, an alternative for reducing the LA toxic side effects and prolonged analgesia is the development of new delivery-systems, is of a great clinical interest.

Poloxamers or Pluronics® (PL), co-polymers composed of basic units of ethylene oxide (OE) and propylene oxide (OP) (Fig. 1B), have been investigated as drug-delivery systems, showing promising results concerned to the improvement of biopharmaceutics, pharmacodynamics and pharmacokinetics properties. PL self-assembly in response to polymer concentration and temperature is the most important aspect to be considered for the development of drug-delivery systems,

* Corresponding author at: Centro de Ciências Naturais e Humanas, Universidade Federal do ABC, UFABC, Av dos Estados, 5001, Bairro Bangú, Bloco A, Torre 3, Sala 623-3, CEP 090210-580 Santo André, SP, Brazil.
*E-mail address:* daniele.araujo@ufabc.edu.br (D.R. de Araujo).

https://doi.org/10.1016/j.ijbiomac.2018.01.064
0141-8130/

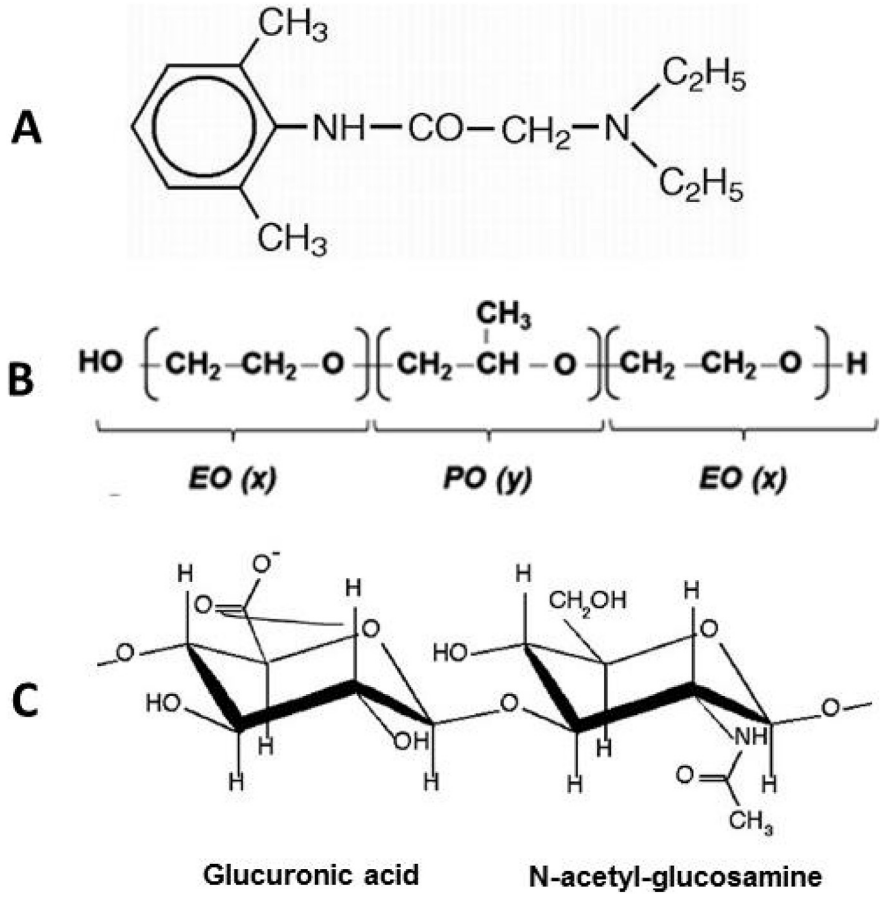


**Fig. 1.** Chemical structures of Lidocaine (A), Pluronic copolymers (B, where x refers to the number of ethylene oxide-EO and y to the propylene oxide units-PO) and hyaluronic acid with its glucuronic acid and *N*-acetyl-glucosamine units (C).

producing high-viscosity hydrogels, due to the transition from the liquid to the soft gel, as a result of micellar aggregation and forming [5,6].

In the last years, the research for biocompatible osteotropic formulations has been presented as a novel approach for the intra-articular injection. Then, the use of hyaluronic acid (HA) (Fig. 1C) offers the possibility of a therapy based on the viscosupplementation. HA is a naturally polysaccharide which belongs to glycosaminoglycans (GAGs) family. It consists of a basic unit of two sugars, glucuronic acid and *N*-acetylglucosamine, polymerized into large macromolecules of over 30,000 repeating units. It is, therefore, one of the largest components of the extracellular matrix of articular cartilage and plays an important role in a variety of cellular processes [7]. HA also acts biochemically, decreasing the gene expression of cytokines and enzymes associated with OA, decreasing the production of prostaglandins and the intra-articular concentration of metalloproteinases. Its presence has an analgesic effect, reducing nerve impulses and sensitivity in nociceptive nerve endings, stabilizing the cartilaginous matrix, stimulating chondrocyte proliferation, increasing type 2 collagen production and chondrocyte

**Table 1**
Temperatures (T), enthalpy ($\Delta H_m$) and Gibb's free energy ($\Delta G°$) relative to the micellization for PL hydrogels.

| Formulations (% m/v) | Additives (% m/v) | $T_{onset}$ (°C) | $T_m$ (°C) | $T_{endset}$ (°C) | $\Delta H_m$ (kJ·mol$^{-1}$) | $\Delta G°$ (kJ·mol$^{-1}$·K) |
|---|---|---|---|---|---|---|
| PLF-127 (20) | – | 13.80 | 17.64 | 30.23 | 52 | −22.81 |
| | LDC | 12.98 | 17.28 | 31.09 | 50 | −22.78 |
| | HA 0.025 | 13.53 | 17.11 | 29.18 | 51.85 | −22.76 |
| | HA 0.025-LDC | 12.95 | 16.15 | 25.46 | 38.90 | −22.70 |
| | HA 0.05 | 13.57 | 17.33 | 29.66 | 54.13 | −22.78 |
| | HA 0.05-LDC | 12.29 | 16.37 | 28.23 | 44.73 | −22.71 |
| PLF-108 (20) | – | 17.92 | 22.38 | 32.28 | 30.62 | −23.55 |
| | LDC | 17.35 | 17.28 | 31.09 | 26.77 | −23.14 |
| | HA 0.025 | 18.85 | 23.10 | 34.00 | 33.18 | −23.60 |
| | HA 0.025-LDC | 17.72 | 22.22 | 33.43 | 36.11 | −23.53 |
| | HA 0.05 | 18.41 | 22.75 | 34.43 | 34.70 | −23.58 |
| | HA 0.05-LDC | 16.77 | 21.16 | 31.04 | 34.38 | −23.45 |
| PLF-127-PLF-108 (10-10) | – | 14.40 | 18.65 | 32.52 | 0.006 | −23.06 |
| | LDC | 14.03 | 18.80 | 29.90 | 0.004 | −23.07 |
| | HA 0.025 | 14.13 | 18.07 | 31.95 | 0.005 | −23.01 |
| | HA 0.025-LDC | 13.27 | 17.36 | 28.09 | 0.004 | −22.95 |
| | HA 0.05 | 14.36 | 18.50 | 31.71 | 0.004 | −23.04 |
| | HA 0.05-LDC | 13.10 | 17.71 | 30.71 | 0.006 | −2298 |

Note: $T_{onset}$ and $T_{endset}$ refer to the initial and final temperatures of the micellization process, respectively. $T_m$ is the peak for micellization process. LDC concentration was (0.2%).

aggregates, and decreasing the degradation of type 2 collagen [8]. Reports in the literature showed that, based on pain relief and improvement on joint function, the effectiveness of intra-articular HA treatment was comparable to that of non-steroidal anti-inflammatory drugs (NSAIDs), highlighting the safety of a local treatment with no systemic action [9]. In fact, different PL and HA hydrogels have been studied for improving rheological and mucoadhesive properties of ocular delivery formulations [10], the incorporation of polycaprolactone microspheres in sodium hyaluronate-PL 407 hydrogels for intradiscal drug-delivery [11] and the synthesis of PL-sodium hyaluronate macromers for delivery applications [12, 13]. However, those studies were devoted to chemical synthesis and formulations composed of one PL-type.

For this study, we have selected the binary system composed of PL F-127 ($PEO_{100}$-$PPO_{70}$-$PEO_{100}$) and PL F-108 ($PEO_{133}$-$PPO_{49}$-$PEO_{133}$). Considering properties such as molecular weight (PL F-108 = 14,600 $g \cdot mol^{-1}$ and PL F-127 = 12,400 $g \cdot mol^{-1}$) and hydrophilic-lipophilic balances (HLB, PL F-127 = 22 and PL F-108 = 28), this system can present differential structures regarding to HA interaction and controlled release profiles due to the presence of PL F-108, a more hydrophilic (~1:5 PPO:PEO ratio) when compared to PL F-127 (~1:3 PPO:PEO ratio). We present here the development and physicochemical characterization of HA-PLF-127/PLF-108 hydrogels associating their thermoreversible properties and the articular extracellular matrix component, for LDC local release. In this context, we have studied the HA-PL systems micellization process, the sol-gel transition, the hydrogels supramolecular organization and, especially, its influence on LDC release profiles and cytotoxicity.

## 2. Experimental methods

### 2.1. PL F-127/PL F-108–HA hydrogels preparation

PL-HA hydrogels were prepared by dispersing HA (0.025 and 0.05% m/v) in PL 407 or PL 108 at 20%, alone or in association PL407-PL108 (10–10% m/v). The PL-HA mixtures were kept at 4 °C under stirring (100 rpm), until the complete dissolution (transparent solution), and

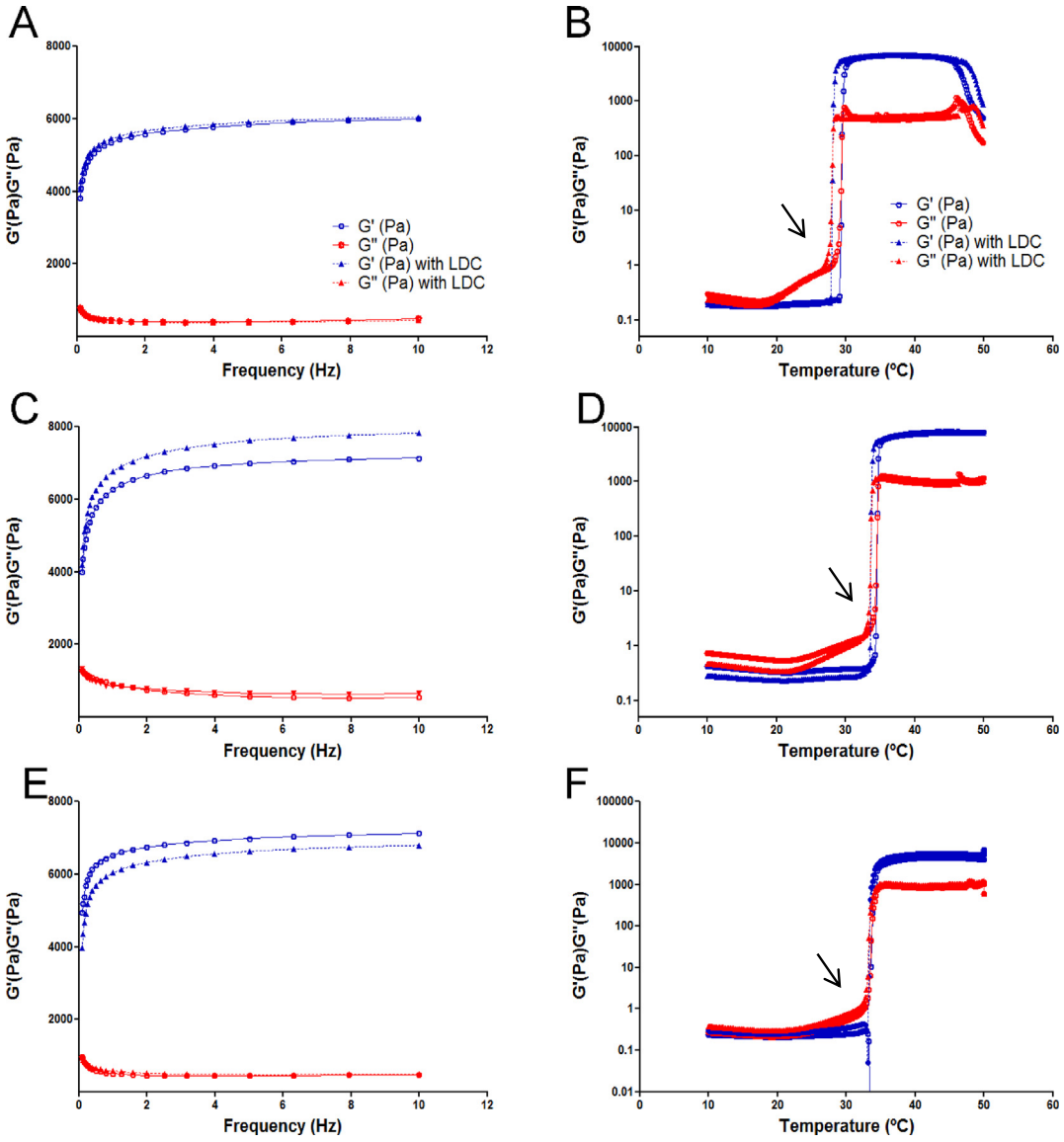


**Fig. 2.** Rheograms presenting frequency sweep analysis (A, C, E) and temperature curves (B, D, F) for the systems containing 0.05% HA: PLF-127 (A, B), PLF-108 (C, D) and PLF-127-PLF-108 (E, F). Arrows indicate the $T_{sol\text{-}gel}$ (sol-gel transition temperature).

**Table 2**
Values referring to the G′ (elastic) and G″ (viscous) moduli, viscosity (η, mPa·s) at 25 °C and 37 °C, sol-gel transition temperatures (Tgel) for each formulation.

| Formulations (% m/v) | Additives (% m/v) | G′ (Pa) | G″ (Pa) | G′/G″ (1 Hz) | η (25 °C) | η (.10$^3$, 37 °C) | Tgel (°C) |
|---|---|---|---|---|---|---|---|
| PLF-127 (20) | – | 10,600 | 573 | 18.5 | 153.2 | 1690 | 27 |
| | LDC | 7870 | 323.9 | 24.3 | 120.4 | 1250 | 26 |
| | HA 0.025 | 6740 | 527.8 | 12.8 | 97.5 | 1076 | 29 |
| | HA 0.025-LDC | 6520 | 448.1 | 14.5 | 87.0 | 1040 | 28 |
| | HA 0.05 | 6890 | 521.8 | 13.2 | 102.6 | 1112 | 29 |
| | HA 0.05-LDC | 6920 | 461.9 | 15 | 104.2 | 1104 | 28 |
| PLF-108 (20) | – | 7190 | 1350 | 5.3 | 42.7 | 1164 | 34 |
| | LDC | 6830 | 1260 | 5.4 | 36.7 | 1105 | 34 |
| | HA 0.025 | 8560 | 1560 | 5.5 | 78.7 | 1384 | 34 |
| | HA 0.025-LDC | 8020 | 1290 | 6.2 | 56.3 | 1266 | 33 |
| | HA 0.05 | 6800 | 1200 | 5.6 | 119 | 1099 | 34 |
| | HA 0.05-LDC | 6810 | 1070 | 6.4 | 86.3 | 1079 | 33 |
| PLF-127-PLF-108 (10-10) | – | 6410 | 1190 | 5.4 | 45.8 | 1038 | 33 |
| | LDC | 6840 | 452.4 | 15.1 | 61.3 | 1090 | 30 |
| | HA 0.025 | 4520 | 1000 | 4.5 | 52.3 | 749.2 | 33 |
| | HA 0.025-LDC | 5970 | 867.2 | 6.9 | 66.5 | 966.1 | 31 |
| | HA 0.05 | 3750 | 907 | 4.1 | 56.4 | 614.6 | 33 |
| | HA 0.05-LDC | 5720 | 912.4 | 6.2 | 72.6 | 910 | 31 |

Note: LDC concentration was (0.2%, in water).

maintained at 8 °C for future use. The LDC base (0.2% m/v) was incorporated in all hydrogels.

### 2.2. Physico-chemical characterization and in vitro release assays

#### 2.2.1. Micellar hydrodynamic diameter

For PL-HA and/or drug-PL interactions studies, the micellar hydrodynamic diameter, mean distribution and polydispersity parameters were determined by Dynamic Light Scattering (DLS). Measurements were performed using a particle analyzer Zetasizer ZS (Malvern®, UK) at a fixed angle of 173 at 25 and 37 °C in order to simulate the micelles behavior at room and body temperatures. PL systems (5% w/v) were filtered through a polycarbonate membrane (pore 0.22 μm), and the measurements were performed at least five times for each sample.

#### 2.2.2. Differential Scanning Calorimetry (DSC) analysis

Differential Scanning Calorimetry (DSC) experiments were performed with a TA Instruments (New Castle, DE) Q-200 DSC apparatus. PL hydrogels were weighed and placed in sealed aluminum pans and analyzed by three successive thermal cycles of heating and cooling (0 to 50 °C, at 5 °C/min), using an empty pan as reference. Thermograms were presented as heat flux (kJ·mol$^{-1}$) *versus* temperature (°C). Thermodynamic parameters such as the Gibbs free energy (ΔG°), enthalpy variation (ΔH°, calculated by the area under the phase-transition peak on the heating cycle), and entropy (ΔS°) were also determined, according to the following equations [6]:

$$\Delta G^{\circ} = RT_{CMT} \ln(x) \quad (1)$$

$$\Delta G^{\circ} = \Delta H - T\Delta S^{\circ} \quad (2)$$

where R is the gas law constant (8.31 J·mol$^{-1}$·K$^{-1}$), T is the micellization temperature (Tm) in K, and x is the PL concentration expressed as mole fraction units.

#### 2.2.3. Rheology

For the sol-gel transition temperature ($T_{sol-gel}$) determination, rheological analyzes were performed by, an oscillatory rheometer (Kinexus Lab., Malvern Instruments) with a cone-plate geometry, using the temperature range from 10 to 50 °C and frequency at 1 Hz. Subsequently, the temperature was set at 37 °C under a frequency sweep from 0.1 to 10 Hz. From the oscillatory measurements were obtained parameters related to the elastic (G′), viscous modulus (G″) and viscosity (η). Data were analyzed by rSpace for Kinexus® software.

#### 2.2.4. Small Angle X-ray Scattering (SAXS) studies

Morphological observations were performed using Small Angle X-ray Scattering (SAXS). The experiments were carried out at the D11A-SAXS1 beamline at the Brazilian Synchrotron Light Laboratory (LNLS) in Brazil. A parallel X-ray beam irradiates a cylindrical sample holder. The radiation wavelength was 1.55 Å and a Pilatus detector at 936 mm distance was used to give a scattering vector ($q = 4\pi/\lambda \sin(\theta)$), where 2θ is the scattering angle ranging from 0.06 to 2.00 nm$^{-1}$. Water scattering curves were collected and subtracted from the samples scattering curve, taking into account its attenuation. All the measurements were performed at 37 °C.

#### 2.2.5. In vitro release assays

*In vitro* release assays were performed using a membrane diffusion model in vertical Franz-type cells with 1.76 cm$^2$ area (Microette Plus®, Hanson Research, CA, USA) with cellulose acetate membranes (MWCO 1000 Da.) as barrier. The donor compartment was filled with 1 g of the hydrogels formulations while the receptor compartment with simulated synovial fluid (NaCl 8 g/L, KCl 0.2 g/L, $NaHPO_4$ 1.44 g/L, $NaH_2PO_4$ 0.24 g/L), pH 7.4, at 37 °C, under magnetic stirring (350 rpm). Aliquots (1 mL) from receptor compartment were withdrawn at intervals from 30 min until 24 h and analyzed by UV–VIS spectrophotometry (λ = 263 nm), using a previously determined calibration curve (y = 0.0654 + 0.455x, LQ = 0.448 mM and LD = 0.147 mM, $R^2 = 0.998$), for determining the LDC concentration.

Release profiles were analyzed according to zero-order, Higuchi, Korsmeyer—Peppas models, as described by following equations, respectively:

$$Q_t = Q_0 + K_0 t \quad (3)$$

where $Q_t$ is the cumulative amount of drug released at time t, $Q_0$ is the initial amount of drug, $K_0$ is the zero-order release constant, and t is time.

$$Q_t = K_H t^{1/2} \quad (4)$$

where the rate of drug release is linear as a function of square root of time and the drug is the only component that diffuses through the medium. In this equation, the release mechanism is described as a diffusion process according to Fick law. $K_H$ is the release coefficient, and $Q_t$ is the drug released amount.

$$M_t/M_\infty = K_{KP} t^n \quad (5)$$

where $M_t/M_\infty$ is the fraction of drug released at time t, $K_{KP}$ is a rate constant, and n is the release exponent. An n value of 0.45 represents Fickian diffusion, 0.45 < n < 0.89 is anomalous (non-Fickian) diffusion, n = 0.89 is case-II transport, and n > 0.89 super case-II transport.

#### 2.2.6. In vitro cytotoxicity evaluation

Vero cell line, established from kidney cells of African green monkey (*Cercopithecus aethiops*) (CCIAL 057, Adolfo Lutz Institute, São Paulo, Brazil), was used for the *in vitro* experiments. Vero cells were cultured in Ham-F-10 medium (Sigma-Aldrich Chem. Co.), with fetal bovine serum (10%; Sigma-Aldrich Chem. Co.), 100 μg/mL penicillin/streptomycin, and maintained at 37 °C with 5% $CO_2$. Assays were performed in triplicate. The tests were performed by direct contact test according to ISO 10993-5 (2009). For the MTT (MTT-3-(4,5-dimethylthiazol-2-

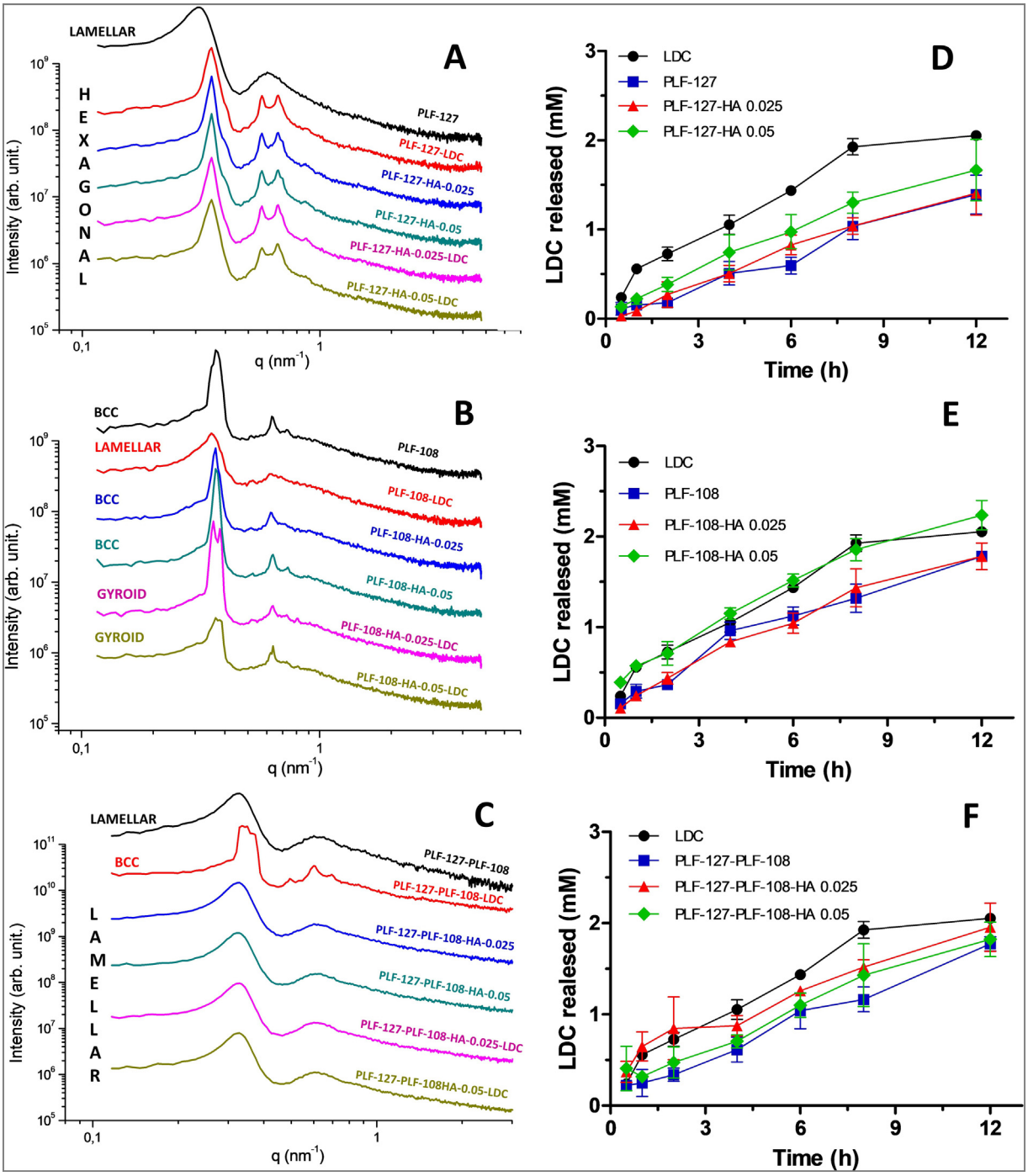


**Fig. 3.** SAXS patterns (at 37 °C; A, B, C) and LDC release profiles (D, E, F) for different PL-based hydrogels before and after HA (0.025 and 0.05%) incorporation. PLF-127 (A and D); PLF-108 (B and E); PLF-127-PLF-108 (C and F).

yl)-2,5-diphenyltetrazolium bromide) assay Vero cells were seeded ($1 \times 10^4$ cells/well) in 96-well plates (TPP). After 24 h, the culture medium was then replaced and 100 μL of the formulations in culture medium was added. After incubation for 24 h, 100 μL of MTT solution (5 mg/mL, in phosphate buffered saline) was added to each well and cells treated for 4 h. After removing the MTT solution, 50 μL of DMSO was added to each well for 10 min, and the absorbance measured at 570 nm. As a negative control, non-cytotoxic, it was only used in and culture medium as described above. As a positive control, cytotoxic, it was used a 0.25% solution of phenol in the described culture medium. For the morphological assay Vero cells, were seeded in 24-well plates (TPP). After 24 h, at a confluence of 80%, forming a monolayer, the culture medium was removed and substituted by hydrogels diluted. The cells were observed by inverted and direct light microscope (A1 Axiovert, Zeiss, Axioscope A1, Zeiss).

### 2.3. Statistical analysis

Each experiment was carried out in triplicate unless otherwise specified. All results are presented as mean ± standard deviation (SD). The experimental data were analyzed using GraphPad Prism software, version 6.0 and Microsoft Excel. For comparisons among more than two groups was used ANOVA (One and TwoWay) and the *post hoc* Tukey

**Table 3**
Structure and lattice parameters (at 37 °C) for different PLF-127, PLF-108 and PLF-127-PLF-108 hydrogels.

| Formulations (% m/v) | Additives (% m/v) | Lattice parameter (nm) | Structure |
|---|---|---|---|
| PLF-127 (20) | – | 20.8 ± 0.1 | Lamellar |
| | LDC | 18.0 ± 0.002 | Hexagonal |
| | HA 0.025 | 17.9 ± 0.03 | Hexagonal |
| | HA 0.025-LDC | 17.9 ± 0.03 | Hexagonal |
| | HA 0.05 | 18.0 ± 0.02 | Hexagonal |
| | HA 0.05-LDC | 18.0 ± 0.03 | Hexagonal |
| PLF-108 (20) | – | 24.0 ± 0.03 | BCC |
| | LDC | 18.3 ± 0.1 | Lamellar |
| | HA 0.025 | 24.4 ± 0.07 | BCC |
| | HA 0.025-LDC | 43.1 ± 0.07 | BCC |
| | HA 0.05 | 24.1 ± 0.03 | BCC |
| | HA 0.05-LDC | 42.4 ± 0.7 | BCC |
| PLF-127-PLF-108 (20) | – | 19.6 ± 0.09 | Lamellar |
| | LDC | 25.7 ± 0.2 | BCC |
| | HA 0.025 | 19.5 ± 0.06 | Lamellar |
| | HA 0.025-LDC | 19.6 ± 0.07 | Lamellar |
| | HA 0.05 | 19.5 ± 0.07 | Lamellar |
| | HA 0.05-LDC | 19.5 ± 0.07 | Lamellar |

Note: BCC – body centered cubic.

test. To comparison between two groups was used the Student's *t*-test. Statistical significance was set at a p-value of ≤.05.

## 3. Results and discussion

### 3.1. Micellar hydrodynamic diameter

Micellar hydrodynamic diameters were determined in order to evaluate the size distribution and interaction drug-micelles for different PLF-127 and/or PLF-108 formulations, before and after HA and/or LDC incorporation. Results present the micellar mean hydrodynamic diameter and the average size distribution for the different systems at 25 °C and 37 °C, simulating a possible dilution of the hydrogel when in contact with biological fluids. At 25 °C, PL F-127 systems presented a bimodal distribution and micellar diameters of 37.4 ± 0.3 nm, as well as a smaller size population of ~5 nm (mean distribution ~ 10 nm) relative to the presence of unimers in solution [6, 14, 15]. On the other hand, PL F-108-based system presented a greater distribution of hydrodynamic diameter of 6.7 ± 0.24 (76.13 ± 1.91%) nm and small populations with larger size (475.6 ± 46 nm). These results are due to differences in HLB and Critical Micellar Temperature (CMT) values for PL F-127 and PL F-108. The HLB value for PL copolymers (whose values are from 1 to 30) characterizes their amphiphilic nature in a dependence on the number PEO and PPO units [15, 16], since high HLB refers to a more hydrophilic copolymer, representing a predominance of PEO units relative to the PPO units (such as in this case for PL F-127, HLB = 22). On the other hand, a low HLB indicates a more lipophilic copolymer, which has lower PEO content than PPO (as observed for PL F-108, HLB = 29) [17]. The differences between PLF-127 and PLF-108 are also observed considering their CMT values (~19.5 and 24.5 °C, for PLF-127 and PLF-108, respectively, explaining the high percentage of monomers for PLF-108 [18].

In the case of binary systems PL F-127/PL F-108, the micellar hydrodynamic diameter and size distribution percentage were similar than that observed for PL F-127-based systems. At 37 °C, it was observed the predominance of a homogeneous systems with unimodal distribution, indicating that the increase in temperature favored the aggregation and leads the formation of mixed micelles with lower values of hydrodynamic diameters (21.71 ± 0.74 and 30.4 ± 3.5 nm). The decrease on micellar diameters, at physiological temperature, can be due to the transition of sol-gel phases and the consequent increase in the viscosity of the formulation caused by the dehydration of PPO units into the micellar core [19, 20].

The presence of HA into the systems provided the formation of aggregates with larger hydrodynamic diameters, proportional to the HA concentration (0.025 and 0.05%). At 37 °C, it was possible to observe average diameters of 26.0 ± 0.75 nm and 42.42 ± 7.54 nm for PLF-127 + HA 0.05% and PLF-108 + HA 0.05%, respectively. This increase on micellar dimensions can be attributed to the high molecular weight of HA (MM = 15KDa), corroborating to the previous work of [10], where the addition of HA at 1 and 2% to PL-based systems led to the formation of larger micellar aggregates. Additionally, the incorporation of the LDC did not, significantly, change the micellar diameters and the polydispersity values for all systems, indicating the homogeneity and organization of the micellar systems.

### 3.2. Differential Scanning Calorimetry (DSC) analysis

Table 1 shows the values for $T_{onset}$, $T_m$ and $T_{endset}$, as well as the enthalpy ($\Delta H_m$) and Gibbs free energy ($\Delta G°$) relative to the micellization process for different associations of HA and PL-based hydrogels. All formulations showed endothermic peaks with a small displacement, which is directly related to the increase of the copolymer concentration and the variations on formulations composition. As also observed by previous studies [6,20], the association kinetics are different since the micelles formation involves the PPO units dehydration and the micelles dissociation are dependent on the PEO units hydration.

DSC analysis showed that the $T_m$, $\Delta H°$ and $\Delta G°$ were similar for all formulations. The $T_m$ values for PLF-127 based systems were from ~12 to 23 °C, according to the PL type and/or the HA incorporation. For PLF-108 systems it was observed a decrease in $\Delta H°$ values, compared to the PLF-127 systems, showing the influence of PLF-108 hydrated micellar corona on micelles self-assembly. However, the binary systems presented more pronounced changes on thermodynamic parameters compared to the PLF-127 formulations. Even considering the different HLB values for PLF-108 (HLB = 28) and PLF-127 (HLB = 22), the association of both PL at 1:1 proportion (PLF-127-PLF-108 at 10:10% m/v) seems to be sufficient to induce conformational changes on micellar

**Table 4**
Release constants and determination coefficients obtained for LDC from different HA-PLF-127, PLF-108 or PLF-127-PLF-108 hydrogels.

| Formulations (% m/v) | Zero order | | Higuchi | | Korsmeyer-Peppas | | |
|---|---|---|---|---|---|---|---|
| | $K_0$ (mM·h$^{-1}$) | $R^2$ | $K_H$ (mM·h$^{-1/2}$) | $R^2$ | $K_{KP}$ (mM·h$^{-n}$) | $R^2$ | n |
| LDC (0.2) | 0.38 ± 0.1 | 0.96 | 0.67 ± 0.05 | 0.98 | 0.46 ± 0.05 | 0.95 | 0.58 |
| PLF-127 (20) | 0.115 ± 0.007 | 0.98 | 0.57 ± 0.06 | 0.96 | 0.15 ± 0.01 | 0.96 | 0.84 |
| PLF-127-HA (20-0.025) | 0.075 ± 0.005 | 0.99 | 0.51 ± 0.05 | 0.96 | 0.1 ± 0.02 | 0.96 | 1.0 |
| PLF-127-HA (20-0.05) | 0.078 ± 0.004 | 0.98 | 0.46 ± 0.02 | 0.94 | 0.18 ± 0.06 | 0.97 | 0.74 |
| PLF-108 (20) | 0.34 ± 0.02 | 0.98 | 0.62 ± 0.02 | 0.96 | 0.28 ± 0.01 | 0.97 | 0.72 |
| PLF-108-HA (20-0.025) | 0.24 ± 0.06 | 0.98 | 0.58 ± 0.02 | 0.93 | 0.24 ± 0.02 | 0.96 | 0.77 |
| PLF-108-HA (20-0.05) | 0.41 ± 0.07 | 0.99 | 0.65 ± 0.02 | 0.95 | 0.56 ± 0.03 | 0.98 | 0.52 |
| PLF-127-PLF-108 (10-10) | 0.33 ± 0.006 | 0.98 | 0.5 ± 0.05 | 0.95 | 0.28 ± 0.01 | 0.95 | 0.66 |
| PLF-127-PLF-108-HA (10-10-0.025) | 0.35 ± 0.06 | 0.98 | 0.41 ± 0.03 | 0.92 | 0.57 ± 0.05 | 0.95 | 0.43 |
| PLF-127-PLF-108-HA (10-10-0.05) | 0.24 ± 0.05 | 0.99 | 0.49 ± 0.02 | 0.95 | 0.41 ± 0.07 | 0.90 | 0.53 |

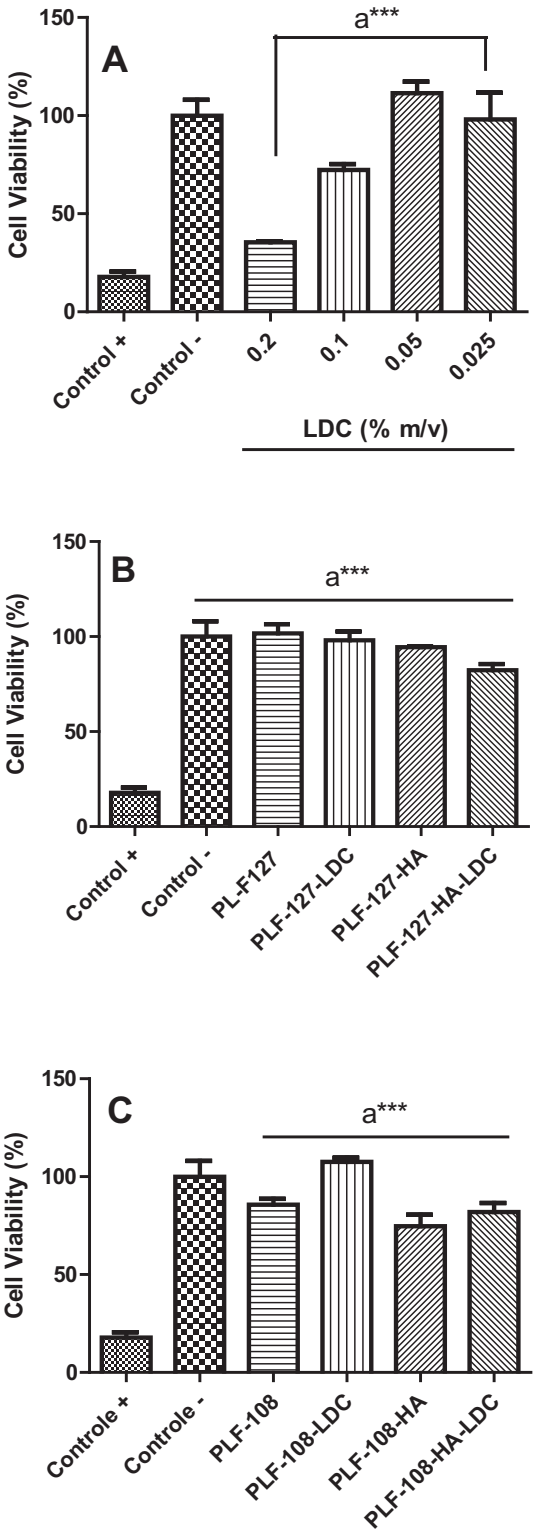


**Fig. 4.** Effects of LDC (A), PL-F127-HA (B) and PLF-108-HA (C) on Vero cells evaluated by MTT reduction test. Positive control (0.25% phenol) and negative control (cells cultured in the culture plate) by MTT assay. Values are reported as mean ± standard deviation (SD) (n = 3). a*** - statistical differences relatively to positive control, ***p < .001.

assembly. In fact, similar results were observed for systems composed of PLF-127 (HLB = 22) and PLF-68 (HLB = 29), where pronounced changes were also reported for enthalpy variation values considering higher PL proportions (2:1 and 5:1) [15]. On the other hand, the presence of different concentrations of HA and LDC incorporation did not have an obvious impact on the micellization temperatures., except for PL-108 (20) based systems, it was observed an increase in the Tm values, which corroborates with the data obtained by DLS, where we noticed the greater influence of the EO: PO ratio of the micellization process [18]. Showing that they do not alter on PL thermoreversible properties even considering different concentrations or formulation compositions.

### 3.3. Rheological analysis

The rheological behavior plays an essential role in PL-based formulations providing information about thermogelling process as a function of frequencies and temperatures variations. In this context, those rheological parameters, such as elastic (G′) and viscous (G″) moduli, viscosity (η) and sol-gel transition temperature (where is observed the most pronounced viscosity variation) were determined for all hydrogels formulations considering the incorporation of HA and/or LDC. All results are presented on Fig. 2 and Table 2.

Fig. 2 shows representative rheograms for hydrogels composed of HA (0.05%) associated to PLF-127 (A and B), PLF-108 (C, D), PLF-127-PLF-108 (E, F), before and after LDC incorporation, under frequency and temperature variation. The incorporation of HA did not shift the $T_{sol-gel}$ obtained for all hydrogels, but differences were observed after comparisons between both PL type, since $T_{sol-gel}$ (~29 °C) values for PLF-127 systems were lower than that observed for PLF-108 and PLF-127-PLF-108 hydrogels (~34 and 33 °C, respectively). Considering that PLF-108 is a more hydrophilic copolymer than PLF-127, the formation of binary systems with PLF-127 evoked a reduction on viscosity values and a possible structural reorganization of the hydrogel, since $T_{sol-gel}$ is dependent on the PL concentration and hydrophobicity [21, 22].

Table 2 shows that at 37 °C (recommended for the development of *in situ* hydrogel systems for injectable use, formulations were structurally liquid-viscous) the values for the elastic modulus (G′) were ~4.1 to 24 times higher than those observed for the viscous modulus (G″), favoring the hydrogels formation. These results are in agreement with the findings in the literature [6, 20], showing that the elastic properties of an injectable hydrogel should predominate over its viscous properties, thereby facilitating the injection [6]. Similarly, published reports revealed an increase in viscosity values, changes of viscoelastic properties and $T_{sol-gel}$ values after the addition of drugs [23, 24].

### 3.4. Hydrogels supramolecular structure: Small Angle X-ray Scattering (SAXS)

The scattering patterns, obtained for all hydrogels before and after HA and/or LDC incorporation are presented on Fig. 3 and lattice parameters are shown on Table 3. All hydrogels presented structural transitions according to the PL-type and incorporation of HA or LDC. In the case of PLF-127 systems, it was observed a transition from lamellar to hexagonal phase while PLF-108 hydrogels phase organization were from body centered cubic (BCC) to gyroid. However, for the binary systems PLF-127-PLF-108 the lamellar phase organization was preserved for the most of formulations.

The effects of HA incorporation were more pronounced for PLF-127 and PLF-108 isolated systems. For the system PLF-127, the addition of both HA concentrations favored and stabilized the transitions from lamellar to hexagonal phase organization, probably due to its interaction with the micellar corona and/or intermicellar spaces. On the other hand, HA did not evoke structural changes on PLF-108 hydrogels, since the BCC organization was maintained for both HA concentrations. Those differences can be attributed to the PLF-108 hydrophilicity and higher OE: OP ratio (5:1) when compared to PLF-127, allowing the HA hydroxyl groups interaction with PL more superficial PEO units. This effect was also observed for the binary system PLF-127-PLF-108, where the lamellar phase organization was preserved after HA addition.

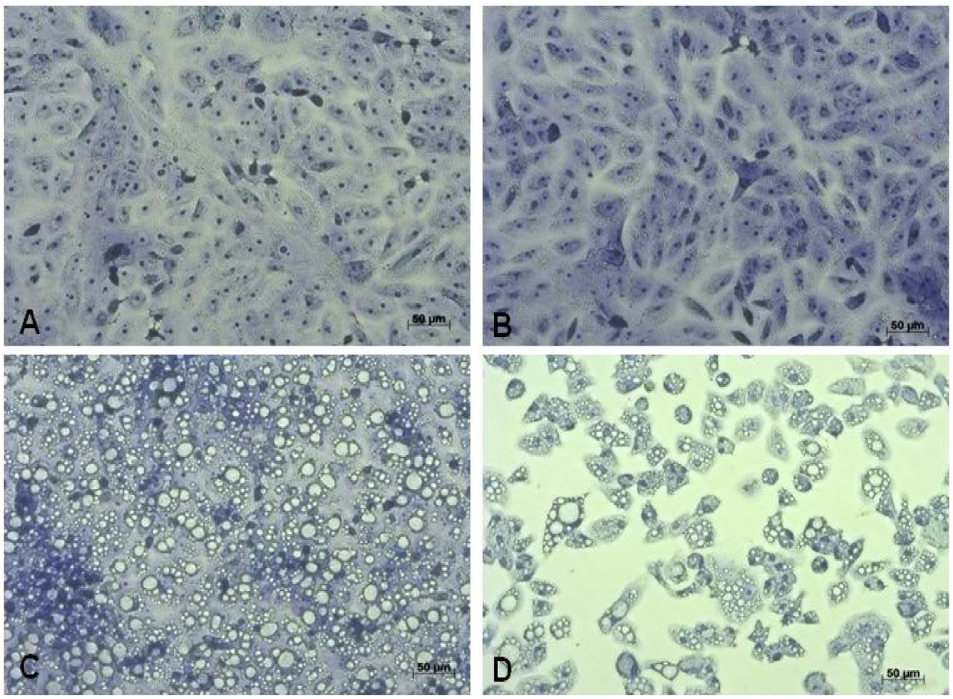


**Fig. 5.** Michrographies obtained after direct cytotoxicity assay. Phase contrast microscopy with toluidine Blue staining for (A) LDC 0.025%; (B) LDC 0.05%; (C) LDC 0.1%; (D) LDC 0.2%. Note the presence of vacuolization and decrease in the number on cells number.

Regarding to LDC addition, structural changes were observed for all hydrogels. In the case of PLF-127-HA and PLF-108-HA, the phase organization was maintained as hexagonal and lamellar, respectively. Those differential effect can be attributed to the possible insertion of LDC base into the micellar core and HA accommodation on the micellar corona. These results suggest that the HA addition favored the structural stabilization of the systems, since in the presence of LDC associated to PL-HA systems, the network parameters are almost unchanged, in a different manner than that observed in the absence for HA. As reported previously [25], when the additives (drugs, salts and other polymers etc.) into the PL systems, new supramolecular can be created due to the formation of "channels" (such as the intermicellar spaces observed for hexagonal and cubic phase organizations) that allow the encapsulation of the drugs. Also, an interesting point is after LDC addition on PLF-108 hydrogels, the network parameter decreased. However, in the presence of HA and after LDC incorporation, the network parameter, for PLF-108 systems, changed from 24.39 ± 0.07 (0.025% HA) to 24.10 ± 0.03 (0.05% HA) and from 43.07 ± 0.07 (0.025% HA) to 42.38 ± 0.66 (0.05% HA). Those differences can be attributed to the PLF-108 higher HLB and molecular weight values (HLB = 28 and MW = 14,600) compared to PLF-127 (HLB = 22 and MW = 12,400), leading to more pronounced hydration effects on the micellar corona surface and a swelling process on BCC structure evoked by HA interference on micellar corona associated to the additional insertion of LDC into the PLF-108 micellar core (Table 3).

### 3.5. In vitro release assays

Fig. 3 and Table 4 show the LDC release profiles from the different formulations. The LDC release in solution (at 0.2% or 8.5 mM, in water) was progressive, reaching a peak at 8 h (2.05 ± 0.05 mM). On the other hand, PLF-127, PLF-108 or PLF-127-PLF-108 formulations evoked a sustained LDC release profile up to ~12 h remaining in a slow progress for all the experiment. The concentrations of LDC released were 1.39 ± 0.02 mM (PLF-127), 1.78 ± 0.03 mM (PLF-108) and 1.77 ± 0.08 mM (PLF-127-PLF-108).

The incorporation of different HA concentrations into the hydrogels reduced the LDC release with more pronounced effects for the system HA-PLF-127 (1.4 ± 0.02 mM and 1.6 ± 0.04 mM, for 0.025 and 0.05% HA, respectively) when compared to HA-PLF-108 and HA-PLF-127-PLF-108 with $p < .01$ for both HA concentrations. The prolongation in the release of LDC through systems containing HA can be attributed to formation of a more closed polymer network. According to literature reports, the addition of a hydrophilic anionic mucopolysaccharide, such as HA, to PL-based hydrogels may cause topological interactions with the other molecules (such as drugs), thus contrasting the release of the same [10, 26, 27].

The analysis of the curves, using mathematical models, such as Zero order, Higuchi and Korsmeyer-Peppas showed differences with related to the LDC release mechanisms, since the highest correlation coefficient values were obtained by fitting curves to the Zero-order model ($0.96 > R^2 > 0.99$). The *in vitro* LDC release value decreased when HA was added to the PLF-127 hydrogel (Krel = 0.075 and 0.078 $mM \cdot h^{-1}$, for 0.25 and 0.5% HA, respectively) when compared to HA-PLF-108 (Krel = 0.24 to 0.41 $mM \cdot h^{-1}$) and HA-PLF-127-PLF-108 (Krel = 0.24 to 0.35 $mM \cdot h^{-1}$), indicating that LDC release from hydrogels is a concentration-independent phenomena.

Different mathematic models describe drug release profiles from immediate and modified release dosage forms. In fact, release mechanisms from some systems can be explained by controlled diffusion or erosion, but most systems present a combination of these mechanisms. In this case, high correlation coefficients were also observed for Higuchi and Korsmeyer-Peppas models, with best fits for Zero-Order model, showing that the LDC release rate was independent of the residual drug concentration. Additionally, for Korsmeyer-Peppas model the *n* values obtained for the most of formulations were from 0.52 to 0.84 (Table 4) being characteristic of anomalous and super case-II kinetics, possibly suggesting a combination of diffusion and erosion for LDC release from hydrogels.

### 3.6. Cytotoxicity assays

Biological assays for evaluating the biocompatibility of pharmaceutical formulations may be carried out through a wide variety of *in vitro*

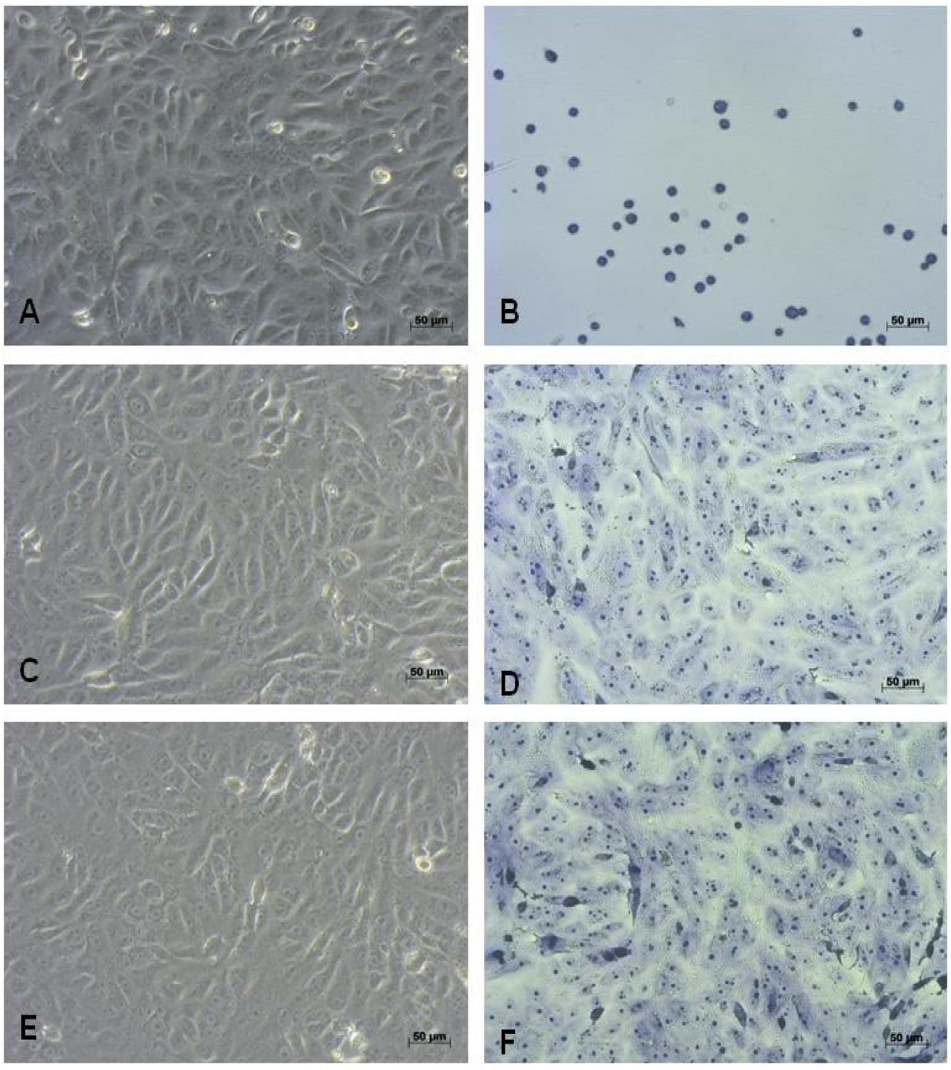


**Fig. 6.** Michrographies obtained after direct cytotoxicity assay. Phase contrast microscopy with toluidine Blue staining for (A) LDC 0.025%; (B) LDC 0.05%; (C) LDC 0.1%; (D) LDC 0.2%. Note the presence of vacuolization and decrease in the number on cells number.

and *in vivo* tests. Such tests may provide useful information regarding the interaction of the system with the physiological environment and the possible risks associated with its application, thus allowing the identification of formulations that do not present characteristics suitable for use in clinical studies [28]. The Vero cells used in cytotoxicity assays represent a standard feature for international studies with biomaterials and have fibroblast like features [29–32].

Cytotoxicity assays were performed by varying concentrations of LDC, PL 407 and PL 108 formulations in the presence and absence of LDC and HA. Cytotoxicity was assessed by MTT reduction (Fig. 4). After 24 h in contact with formulations, the cells were observed for their morphology by phase contrast microscopy and stained with toluidine (Figs. 5 and 6).

Cell viability assays for PLF-127 and PLF-108 in the presence or absence of HA or LDC did not show toxicity to the Vero cells. The percentage of cell viability for PLF-127 systems ranged from 100% for the system isolated to ~90% in the presence of HA and LDC. Whereas for the PLF-108 systems cell viability was from 90 to 80% (Fig. 4). These results demonstrate that the formulations analyzed present no statistical difference in relation to the negative control showing no cytotoxicity to the Vero cells. In the case of LDC, it was observed that the mean percentages of cell viability ranged from 86% to 35% of the lowest (0.02%) for the highest (0.2%) LDC concentrations, respectively. This result shows that the isolated drug tested in the higher concentration showed cytotoxicity while this same concentration carried in the release systems presented cellular viability above 80%.

In Fig. 5 we observed the cell viability percentage for different concentrations of LDC when in contact with Vero cells. In the case of 0.1 and 0.2% concentrations, the presence of vacuolization and decrease in the number of cells can be noted, resulting from drug toxicity.

Those results were also confirmed using q qualitative morphologic assay. The negative, non-cytotoxic control presented a confluent monolayer of cells, typically fibroblastic-like, according to the growth pattern of Vero cells. The cells were quite scattered and elongated, without the presence of cellular debris or evidence of cell degeneration. In the positive control (phenol 0.25%) the presence of few cells and debris, were observed, typical characteristics of cytotoxicity. Fig. 6 shows the cytotoxicity results of the cells in contact with the PLF-127-HA 0.05%-LDC and PLF-108-HA 0.05%-LDC. In all cases, cells presented a growth pattern similar to that obtained with the negative, non-cytotoxic control, without changes in their morphology, such as vacuolization or signs of cell degeneration, and forming a confluent monolayer.

## 4. Final considerations and perspectives

Most articular surgeries (hip, knee, ankle, elbow, shoulder etc.) are usually performed when medical or conventional non-surgical procedures treatment has not diminished the patient symptoms for

improving the motor function in the affected joint. Those surgeries involve joint resection and interpositional reconstruction. For joint resection, a portion of the bone is removed from a stiffened joint, increasing the space between the bone and the socket to improve the range of motion. Scar tissue eventually fills the gap, narrowing joint space again. In those cases, pain relief is achieved and joint motion is restored, but with less stability. On the other hand, interpositional reconstruction reshapes the joint and inserts a prosthetic disk between the two bones, forming the joint. When this reconstruction fails, total joint replacement may be necessary, remaining a long and painful post-operative period [1,3].

In this context, the intra-articular injection of HA (viscosupplementation) has been reported as an effective therapeutic approach to restoring the viscoelasticity of the synovial joint, as a lubricant and shock absorber during joints movement. Those effects are attributed to its unique rheological properties (related to a high-molecular weight in a gel formulation), which the main clinical benefits are: i) reduction of the articular friction; ii) chondroprotection during mechanical stress; iii) induction of proteoglycan and glycosaminoglycan synthesis, as well as anti-inflammatory and analgesic actions [33]. All those features can be also useful for patient recovery after arthroplasties.

Here, we presented the development of different hydrogels associating the HA viscoelastic with PL thermosensitive properties. In special, we reported the influence of viscoelastic features, inherent to HA, on supramolecular structure of PL-based hydrogels and its consequent effects on drug release. In fact, after HA incorporation, PL hydrogels presented similar $T_{sol\text{-}gel}$ temperatures and no interference on PL-thermoreversible properties was observed. However, the HA pronounced structural effect was observed on drug release profiles, since lower release constants were observed for the system HA-PLF-127, that presented a hexagonal phase organization, as observed by SAXS patterns. Additionally, when the HA concentration was raised from 0.025 to 0.05%, the drug release was faster when compared to the other formulations. Those different behaviors seem to be a result of the influence of HA insertion into the systems composed of PLF-108, more hydrophilic compared to PLF-127, leading to phase organization transitions from BCC to gyroid and/or from BCC to lamellar, as observed for the binary hydrogels (HA-PLF-127-PLF-108). However, those phase transitions were not associated to lower release constants, showing that the hexagonal phase organization is essential for a sustained drug release performance. Finally, the evaluation of cytotoxicity showed that the hydrogels formulation containing HA and/or LDC, were non-cytotoxic to the VERO cells. Those results pointed out the tendency to self-assembly of the systems based on HA-PL and their possible application as drug delivery systems.

## Acknowledgements

This research work was supported by Coordenação de Aperfeiçoamento de Pessoal de Nível Superior (CAPES 00.889.834/0001-08), Fundação de Amparo à Pesquisa do Estado de São Paulo (FAPESP 2014/26200-9, 2014/14457-5, 2015/14763-1) and Conselho Nacional de Desenvolvimento Científico e Tecnológico (CNPq 309207/2016-9, 402838/2016-5). We are also grateful to the Brazilian Synchrotron Light Laboratory for SAXS facilities (SAXS 1 beamline).

## References

[1] A.H. Zugliani, N. Verçosa, J.L.G. Amaral, L. Barrucand, C. Salgado, M.B.H. Karam, Control of postoperative pain following total knee arthroplasty: is it necessary to associate sciatic nerve block to femoral nerve block? Rev. Bras. Anestesiol. 57 (2007) 514–524.
[2] A. Tatai, Z. Aigner, I. Eros, M. Kata, Preparation and investigation of mixtures containing lidocaine base and b-cyclodextrin, J. Incl. Phenom. Macrocycl. Chem. 59 (2007) 105–113.
[3] T.H. Lui, Arthroscopic interpositional arthroplasty of the second metatarsophalangeal joint, Arthrosc. Tech. 5 (2016) 1333–1338.
[4] A.D. Hansen, J.A. Rand, Evaluation and treatment of infection at the site of a total hip or knee arthroplasty, J. Bone Joint Surg. Am. 80 (1998) 910–922.
[5] G. Dumortier, J.L. Grossiord, F. Agnely, J.C. Chaumeil, A review of poloxamer 407 pharmaceutical and pharmacological characteristics, Pharm. Res. 23 (2006) 2709–2728.
[6] A. Oshiro, D.C. da Silva, J.C. de Mello, V.W.R. de Moraes, L.P. Cavalcanti, M.K.K.D. Franco, M.I. Alkschbirs, L.F. Fraceto, F. Yokaichiya, T. Rodrigues, D.R. de Araujo, Pluronics f-127/l-81 binary hydrogels as drug-delivery systems: influence of physicochemical aspects on release kinetics and cytotoxicity, Langmuir 30 (2014) 13689–13698.
[7] R.D. Price, M.G. Berry, H.A. Navsari, Hyaluronic acid: the scientific and clinical evidence, J. Plast. Reconstr. Aesthet. Surg. 60 (2007) 1110–1119.
[8] W. Zhang, R.W. Moskowitz, G. Nuki, OARSI recommendations for the management of hip and knee osteoarthritis, part II: OARSI evidence-based, expert consensus guidelines, Osteoarthr. Cartil. 16 (2008) 137–162.
[9] T. Iannitti, D. Lodi, B. Palmieri, Intra-articular injections for the treatment of osteoarthritis: focus on the clinical use of hyaluronic acid, Drugs R&D 11 (2011) 13–27.
[10] L. Mayol, M. Biondi, F. Quaglia, S. Fusco, A. Borzacchiello, L.A. Ambrosio, M.I. Rotonda, Injectable thermally responsive Mucoadhesive gel for sustained protein delivery, Biomacromolecules 12 (2011) 28–33.
[11] J.W. Lee, T.H. Lim, J.B. Park, Intradiscal drug delivery system for the treatment of low back pain, J. Biomed. Mater. Res. A 92 (2010) 378–385.
[12] S.H. Hsu, Y.L. Leu, J.W. Hu, J.Y. Fang, Physicochemical characterization and drug release of thermosensitive hydrogels composed of a hyaluronic acid/pluronic f127 graft, Chem. Pharm. Bull. 57 (2009) 453–458.
[13] H.W. Huh, L. Zhao, S.Y. Kim, Biomineralized biomimetic organic/inorganic hybrid hydrogels based on hyaluronic acid and poloxamer, Carbohydr. Polym. 126 (2015) 130–140.
[14] L. Gentile, G. de Luca, F.E. Antunes, C.O. Rossi, G.A. Ranieri, Thermogelation analysis of F127-water mixtures by physical chemistry techniques, Appl. Rheol. 20 (2010) 1–3.
[15] A.C.S. Akkari, E.V.R. Campos, A.F. Kepler, L.F. Fraceto, E. de Paula, G.R.D.R. de Araujo, Colloids Surf. B: Biointerfaces 138 (2016) 138–147.
[16] S. Fusco, A. Borzacchiello, P.A. Netti, Perspectives on: PEO-PPO-PEO triblock copolymers and their biomedical applications, J. Bioact. Compat. Polym. 21 (2006) 149–164.
[17] M.Y. Kozlov, N.S. Melik-Nubarov, E. Batrakova, Relationship between pluronic block copolymer structure, critical micellization concentration and partitioning coefficients of low molecular mass solutes, Macromolecules 33 (2000) 3305–3313.
[18] P. Alexandridis, J.F. Holzwarthf, T.A. Hatton, Micellization of poly(ethy1ene oxide)-poly(propy1ene oxide)-poly(ethy1ene oxide) triblock copolymers in aqueous solutions: thermodynamics of copolymer association, Macromolecules 27 (1994) 2414–2425.
[19] H.Y. Yang, Z. Shicheng, L. He, X. Xiaoyun, Z. Jing, H. Pingsheng, Studies on the micellization and intermicellar interaction of CTAB in dilute solution, J. Mater. Sci. 40 (2005) 4645–4648.
[20] Y. Zhang, Y.M. Lam, W.S. Tan, Poly(ethylene oxide)-poly(propylene oxide)-poly(ethylene oxide)-g-poly(vinylpyrrolidone): association behavior in aqueous solution and interaction with anionic surfactants, J. Colloid Interface Sci. 285 (2005) 74–79.
[21] K. Edsman, J. Carlfors, R. Petersson, Rheological evaluation of poloxamer as an in situ gel for ophthalmic use, Eur. J. Pharm. Sci. 6 (1998) 105–112.
[22] G.G. Pereira, F.A. Dimer, S.S. Guterres, C.P. Kechinski, J.E. Granada, N.S.M. Cardozo, Formulation and characterization of poloxamer 407: thermoreversible gel containing polymeric microparticles and hyaluronic acid, Quim Nova 36 (2013) 1121–1125.
[23] E.J. Ricci, M.V.L.B. Bentley, M. Farah, R.E.S. Bretas, J.M. Marchetti, Rheological characterization of Poloxamer 407 lidocaine hydrochloride gels, Eur. J. Pharm. Sci. 17 (2002) 161−167.
[24] M.N. Freitas, M. Farah, R.E.S. Bretas, E. Ricci-Júnior, J.M. Marchetti, Rheological characterization of Poloxamer 407 nimesulide gels, Rev. Ciências Farm. Básica e Apl. 27 (2009) 113–118.
[25] M. Salim, W.F.N.W. Iskandar, M. Patrick, N. Idayu Zalid, R. Hashim, Swelling of bicontinuous cubic phases in guerbet glycolipid: effects of additives, Langmuir 32 (2016) 5552−5561.
[26] L. Ambrosio, A.P.A. Borzacchiello, N.L. Netti, Properties of new materials: rheological study on hyaluronic acid and its derivative solutions, J. Macromol. Sci., Pure Appl. Chem. 36 (1999) 991–1000.
[27] L. Mayol, M. Biondi, F. Quaglia, S. Fusco, A. Borzacchiello, L.A. Ambrosio, M.I. Rotonda, A novel poloxamers/hyaluronic acid in situ forming hydrogel for drug delivery: rheological, mucoadhesive and in vitro release properties, Eur. J. Pharm. Biopharm. 70 (2008) 199–206.
[28] S.O. Rogero, A.B. Lugão, T.I. Ikeda, Á.S. Cruz, Teste *in vitro* de citotoxicidade: estudo comparativo entre duas metodologias, Mater. Res. 6 (2003) 317–320.
[29] C.B. Lombello, S.M. Malmonge, M.L. Wada, PolyHEMA and polyHEMApoly(MMA-co-AA) as biomaterials for culturing Vero cells, J. Mater. Sci. Mater. Med. 11 (2000) 541–546.
[30] J.R. Santos, S.H. Barbanti, E.A.R. Duek, H. Dolder, R.S. Wada, M.L.F. Wada, Vero cell growth and differentiation on poly (L-lactic acid) membranes of different pore diameters, Artif. Organs (1) (2001) 7–13.
[31] H.S. Costa, E.F. Stancioli, M.M. Pereira, R.L. Oréfice, H.S. Mansur, Synthesis, neutralization and blocking procedures of organic/inorganic hybrid scaffolds for bone tissue engineering applications, J. Mater. Sci. Mater. Med. (2) (2009) 529–535.
[32] R.Y. Li, Z.G. Liu, H.Q. Liu, L. Chen, J.F. Liu, Y.H. Pan, Evaluation of biocompatibility and toxicity of biodegradable poly (DL-lactic acid) films, Am. J. Transl. Res. 8 (2015) 1357–1370.
[33] R.C. Machado, S. Capela, F.A.C. Rocha, Polysaccharides as viscosupplementation agents: structural molecular characteristics but not rheology appear crucial to the therapeutic response, Front. Med. 4 (2017) 82–86.